

MIT Open Access Articles

*This is a supplemental file for an item in DSpace@MIT*

**Item title:** Backbone resonance assignment for the N-terminal region of bacterial tRNA-(N1G37) methyltransferase

**Link back to the item:** <https://hdl.handle.net/1721.1/125955>



# **Backbone resonance assignment for the full length tRNA-(N<sup>1</sup>G37)**

## **methytransferase of *Pseudomonas aeruginosa***

Yan Li<sup>1,6,7</sup>, Wenhe Zhong<sup>2,3,6</sup>, Ann Zhufang Koay<sup>1</sup>, Hui Qi Ng<sup>1</sup>, Qianhui Nah<sup>2</sup>, Yee Hwa Wong<sup>3,4</sup>, Jeffrey Hill<sup>1</sup>, Julien Lescar<sup>3,4\*</sup>, & Peter C. Dedon<sup>2,5,\*</sup>, CongBao Kang<sup>1,\*</sup>,

<sup>1</sup>Experimental Drug Development Centre, 31 Biopolis Way, #03-01 Nanos, Singapore 138669, Singapore.

<sup>2</sup>Infectious Disease and Antimicrobial Resistance Interdisciplinary Research Groups, Singapore-MIT Alliance for Research and Technology, 1 CREATE Way, 138602, Singapore

<sup>3</sup>NTU Institute of Structural Biology, Nanyang Technological University, 636921, Singapore

<sup>4</sup>School of Biological Sciences, Nanyang Technological University, 60 Nanyang Drive, 637551, Singapore

<sup>5</sup>Department of Biological Engineering, Massachusetts Institute of Technology, Cambridge, MA 02139, USA.

<sup>6</sup>These authors contributed equally to this work.

<sup>7</sup>Current address: Department of Pathogen Biology, School of Basic Medicine, Tongji Medical College, Huazhong University of Science and Technology, 13 Hangkong Road, Wuhan, Hubei, P.R.China, 430030

\*Correspondence should be addressed to Julien Lescar (julien@ntu.edu.sg), P.C.D. (pcdedon@mit.edu) or C.K. (cbkang@eddc.a-star.edu.sg).

## **Abstract**

Bacterial tRNA (guanine37-N<sup>1</sup>)-methyltransferase (TrmD) plays important roles in translation, making it an important target for the development of new antibacterial compounds. TrmD comprises two domains with the N-terminal domain binding to the S-adenosyl-L-methionine (SAM) cofactor and the C-terminal domain critical for tRNA binding. Bacterial TrmD is functional as a dimer. Here we report the backbone NMR resonance assignments for the full length TrmD protein of *Pseudomonas aeruginosa*. Most resonances were assigned and the secondary structure for each amino acid was determined according to the assigned backbone resonances. The availability of the assignment will be valuable for exploring molecular interactions of TrmD with ligands, inhibitors and tRNA.

**Keywords:** TrmD · *Pseudomonas aeruginosa* · tRNA methyltransferase · epitranscriptome · drug discovery · antibacterial · protein dynamics · backbone assignment

## Biological content

Methylation of guanine at position 37 in RNA is critical for bacterial growth, as this reaction is essential for preventing reading frame shifts during translation and therefore for maintaining the fidelity of protein synthesis (Bjork, Wikstrom and Bystrom 1989). This methylation is catalyzed by the tRNA (guanine37-N<sup>1</sup>)-methyltransferase (TrmD). TrmD uses S-adenosyl-L-methionine (SAM) as a cofactor and transfers the methyl group to the N<sup>1</sup> atom of G37 in tRNA (O'Dwyer et al. 2004). TrmD has been shown to be critical for growth of bacteria such as *Pseudomonas aeruginosa* (Jaroensuk et al. 2019), *Escherichia coli* (Persson et al. 1995) and *Streptococcus pneumoniae* (Thanassi et al. 2002, O'Dwyer et al. 2004). Although methylation at G37 is conserved among eukaryotes, archaea and bacteria (Juhling et al. 2009), structural studies and biochemical analysis suggests that bacterial TrmD and eukaryotic tRNA methyltransferase 5 (Trm5) originated from different ancestral enzymes (Goto-Ito, Ito and Yokoyama 2017). In agreement with this hypothesis, the folding of the SAM binding site differs between eukaryotic and bacterial methyltransferase (Goto-Ito et al. 2009), suggesting that it should be, in principle, possible to develop specific inhibitors that will not cross-react with the human methyltransferase. Therefore, bacterial TrmD protein appears as an attractive antibacterial target and efforts have been spent to develop potent inhibitors (Hill et al. 2013). *P. aeruginosa* is an important human pathogen and its TrmD is a validated drug target (Hill et al. 2013 and Jaroensuk et al. 2019). Structural studies on bacterial TrmD will be helpful for structure-based drug discovery programs. The three-dimensional structure of TrmD was initially reported using X-ray crystallography, in the presence of the SAM cofactor and also as a ternary complex with tRNA (Ito et al. 2015, Thomas et al. 2011). Bacterial TrmD was found to contain an N-terminal domain (NTD) responsible for SAM binding, a short linker and a C-terminal domain (CTD) important for tRNA

binding. TrmD functions as a homodimer in which both the N- and C-terminal domains are involved in forming the 2-fold symmetric dimerization interface. We recently reported that the N-terminal domain alone is able to form dimers in solution and exhibits molecular interactions with SAM or SAM competitive inhibitors (Li et al. 2018, Zhong et al. 2019). This was consistent with the previous observation that the NTD binds to SAM and to some competitive inhibitors such as sinefungin (SFG) (Holmes, Andraos-Selim and Redlak 1995).

Here, we carried out solution NMR studies on the full length TrmD of *P. aeruginosa*. The full length *Pa*TrmD harbours 252 amino acids and exists as a dimer in solution. We obtained chemical shift assignments for the backbone resonance of *Pa*TrmD. Secondary structural analysis based on the assigned resonances was carried out and the secondary structure appears very similar to that of the *Pa*TrmD crystal structure (PDB accession code: 5WYQ). We found that the purified *Pa*TrmD exhibited molecular interactions with SAM and its analogues resulting in a significant increase of protein thermal stability. The availability of backbone resonance assignments for the full length TrmD protein will facilitate further studies on TrmD interactions with various ligands.

## **Materials and methods**

### **Protein purification**

The cDNA encoding the full length TrmD of *Pseudomonas aeruginosa* was cloned into the *Nde I* and *Xho I* sites of pET29b. The resulting plasmid encodes a protein with a hexa-histidine tag at the C-terminus. To express the full length TrmD for NMR studies, the plasmid was transformed into *E. coli* BL21(DE3) competent cells. The recombinant protein was produced under the same conditions as those used for the N-terminal domain of TrmD (Li et al. 2018). The induction condition was 18 °C in the presence of 0.5 mM IPTG overnight. To get high protein expression,

the IPTG was added to the culture when the cell density ( $OD_{600}$ ) reached 0.6-0.8. Isotopically labeled proteins were produced by growing the cells in M9 medium supplied with 2 g L<sup>-1</sup> <sup>13</sup>C-glucose, 1 g L<sup>-1</sup> <sup>15</sup>NH<sub>4</sub>Cl and 100% D<sub>2</sub>O. The cells with induced protein were harvested by centrifugation at 7000 ×g, 4 °C for 10 min. The cells were lysed using a sonicator in a buffer containing 20 mM sodium phosphate, pH 7.8, 500 mM NaCl, and 2 mM β-mercaptoethanol in an ice bath. The resulting cell lysate was cleared by centrifugation at 40,000 × g 4 °C, for 20 min before loading onto a gravity column with Ni<sup>2+</sup>-NTA affinity resin. The resin was then washed with a buffer containing 20 mM sodium phosphate, pH 7.2, 1 M NaCl, 20 mM imidazole and 2 mM β-mercaptoethanol. TrmD was then eluted from the resin using an elution buffer containing 500 mM imidazole, 500 mM NaCl at pH 6.5, and 2 mM β-mercaptoethanol. The purified fractions were further loaded onto a HiPrep™ 16/60 sephacryl™ S-200 HR column in a buffer that contained 20 mM sodium phosphate, pH 7.2, 150 mM KCl, 0.5 mM EDTA and 1 mM DTT. Fractions were combined and concentrated to 0.8-1.2 mM with an Amicon Centrifugal Filter unit with a molecular weight cutoff of 3 kDa for NMR data acquisition. In addition, the native *Pa*TrmD protein used for the thermal stability assay was expressed and purified as described previously (Li et al. 2018, Zhong et al. 2019). The <sup>1</sup>H-<sup>15</sup>N-HSQC spectra of <sup>15</sup>N-labeled and <sup>15</sup>H/<sup>13</sup>C/<sup>2</sup>H-labeled *Pa*TrmD were very similar, indicating complete back exchange of the HN in the deuterated medium.

### **Thermal stability assay**

The thermal stability analysis was performed as described for the N-terminal domain of *Pa*TrmD (Li et al. 2018). Briefly, the assay was carried out in a 96-well PCR plate (Bio-Rad) with a volume of 50 µl per reaction containing 5× SYPRO Orange dye (Invitrogen), 4 µM of test

protein and 0.5 mM of test ligand(s) (SAM, S-adenosylhomocystein (SAH), and methylthioadenosin (MTA)) or 1 mM sinefungin (SFG). 0.9% (v/v) DMSO was present when SFG was tested for optimal solubility of the test compound. To serve as negative controls, assay buffer only (50 mM Tris-HCl pH 8.0, 150 mM NaCl, 1 mM MgCl<sub>2</sub>, 1 mM DTT and 0.05% Tween-20) or assay buffer containing 0.9% DMSO was added in place of the test ligand. A linear 25 to 95 °C temperature gradient was applied on the samples in an i-Cycler iQ5 real-time PCR (Bio-Rad). Thermal stability curves and the temperature midpoint  $T_m$  for protein-unfolding transitions were analysed using the Bio-Rad iQ5 software.

### **Backbone resonance assignment**

A <sup>13</sup>C, <sup>15</sup>N, <sup>2</sup>H-labeled TrmD was used for backbone data acquisition using the experiment protocol described previously (Zhang et al. 2016, Gayen, Li and Kang 2012). The following experiments including 2D-<sup>1</sup>H-<sup>15</sup>N-HSQC, transverse relaxation-optimized spectroscopy (TROSY) (Pervushin et al. 1998, Salzmänn et al. 1998)-based 3D- HNCA, HN(CO)CA, HN(CO)CACB, HNCACB, HNCO, HNCACO and NOESY-TROSY (mixing time 120 ms) were collected and processed for obtaining the backbone resonance assignment (Li et al. 2016, Kim et al. 2013, Li, Raida and Kang 2010). All NMR experiments were conducted at 37 °C on a Bruker Avance 600 MHz or 700 MHz spectrometer equipped with a cryoprobe. All spectra were acquired using Topspin (version 2.1). The data were processed with NMRPipe (Delaglio et al. 1995) and Topspin (version 2.1). The peak lists were picked and analyzed using NMRView (Johnson 2004) or CARA (<http://wiki.cara.nmr.ch/FrontPage>). Secondary structure predictions of the TrmD were carried out using TALOS+ based on the chemical shifts of the backbone resonances (Shen et al. 2009).

## Assignments and data deposition

The full length *PaTrmD* could be purified for solution NMR studies. The native *PaTrmD* protein contains 252 amino acids and the purified recombinant protein exists as a dimer in solution (Zhong et al. 2019).  $^{13}\text{C}$ ,  $^{15}\text{N}$ ,  $^2\text{H}$ -labeled *PaTrmD* exhibited detectable cross peaks in the  $^1\text{H}$ - $^{15}\text{N}$ -HSQC spectrum (**Fig. 1**), indicating that it is feasible to conduct backbone resonance assignment experiments. The chemical shifts of the backbone resonances including  $^{13}\text{C}\alpha$ ,  $^{15}\text{N}$ ,  $^1\text{HN}$  and  $^{13}\text{C}'$  were obtained using TROSY-based hetero-nuclear NMR experiments based on the connectivity of the  $\text{C}\alpha$  and  $\text{C}\beta$  chemical shifts and help of the TROSY-NOESY experiment. The recombinant *PaTrmD* construct used in the current study contains 258 residues including eleven proline amino acids and a six-histidine tag at the C-terminus. Most cross peaks (223/242) in the  $^1\text{H}$ - $^{15}\text{N}$ -HSQC spectrum were assigned (Fig. 1). Amino acids that could not be assigned include M1, D2, T38, F58, K67, L71, G84, Y120, G122, T187, R188, A193, I209, R210, R211, W212, G236 and S252. Excluding the six histidine residues at the C-terminus, 90% (a total of 227 out of 252) of  $^{13}\text{C}\alpha$  and 84% (a total of 193 out of 229) of  $^{13}\text{C}\beta$  were assigned. The  $^1\text{H}$ - $^{15}\text{N}$ -HSQC spectrum from the NTD (Li et al. 2018) overlaps well with that of the full length *PaTrmD* (Fig. 2A), which helps assignment for the complete protein. Some residues exhibited low peak intensities in the  $^1\text{H}$ - $^{15}\text{N}$ -HSQC spectrum, which might be due to exchange in the structure. Some cross peaks in the  $^1\text{H}$ - $^{15}\text{N}$ -HSQC spectrum could not be unambiguously assigned, which might be due to multiple conformations of some residues. The chemical shift assignments for the full length *PaTrmD* have been deposited in the BioMagResBank under accession number 27619.

Secondary structures for the assigned residues of *PaTrmD* were analyzed using TALOS+(Shen et al. 2009) and TALOS-N (Shen and Bax 2013). The secondary structures



obtained are similar to those derived from X-ray crystallography (PDB accession code: 5WYQ, Fig. 2B) except for some slight differences. In the X-ray structure, the N-terminal domain of *PaTrmD* was shown to have five  $\beta$ - strands and seven  $\alpha$ -helices and the C-terminal domain is formed by several helices (**Fig. 2C**). Secondary structure prediction reveals that the N-terminal domain of *PaTrmD* contains five  $\beta$ -strands including  $\beta$ 1 (spanning residues R4-V10),  $\beta$ 2 (L35-W40),  $\beta$ 3 (K88-L92),  $\beta$ 4 (A112-A117), and  $\beta$ 5 (E134-S137). The six identified  $\alpha$ -helices in the N-terminal domain include  $\alpha$ 1 (spanning residues E15-A19),  $\alpha$ 2 (I25-K31),  $\alpha$ 3 (E72-A82),  $\alpha$ 4 (Q101-A108),  $\alpha$ 5 (E125-H131), and  $\alpha$ 6 (E147-L160) (Fig. 2C). The C-terminal region of *PaTrmD* contains four helices including  $\alpha$ 7 (E199-L201),  $\alpha$ 8 (R213-G219, W222-R224),  $\alpha$ 9 (A226-S231), and  $\alpha$ 10 (E237-R249). The secondary structures of *PaTrmD* in solution are similar to those seen in the X-ray structure, except that in solution,  $\alpha$ 8 is shorter and R220-T221 are predicted to be unstructured in solution (Fig. 2C). Missing assignments of residues such as I209-W212 accounted for the short length of  $\alpha$ 8, which also suggested that there might be exchange in this region. The linker region between NTD and the C-terminal region is flexible in the X-ray structure. NMR study suggested that residues in this region were not structured while some amino acids were more stable than those in the loop of NTD (Fig. 2C). This might be due to their involvement in protein dimerization in solution. As was observed for the NTD, the active-site ligands including SAM, SAH, MTA and SFG significantly enhanced the thermostability of full length *PaTrmD* by binding to the active site (Fig. 3). Therefore, the current NMR assignments will enable us to carry out ligand binding studies which will assist drug discovery efforts.

**Acknowledgements**

CK appreciates the support from NMRC OF-IRG grant (NMRC/OFIRG/0051/2017) and A\*STAR JCO grant (1431AFG102/1331A028). This work is also supported by National Research Foundation of Singapore through the Singapore-MIT-Alliance for Research and Technology (SMART) Infectious Disease and Antimicrobial Resistance Interdisciplinary Research Groups. W.Z. was supported by a SMART Scholar Fellowship. We also thank Prof Ho Sup Yoon and Dr. Hong Ye from Nanyang Technological University for the NMR experiments. The authors appreciate the valuable discussion from the team members at EDDC, A\*STAR.

**Conflict of interest**

The authors declare that they have no conflict of interest.

## Figure Legends

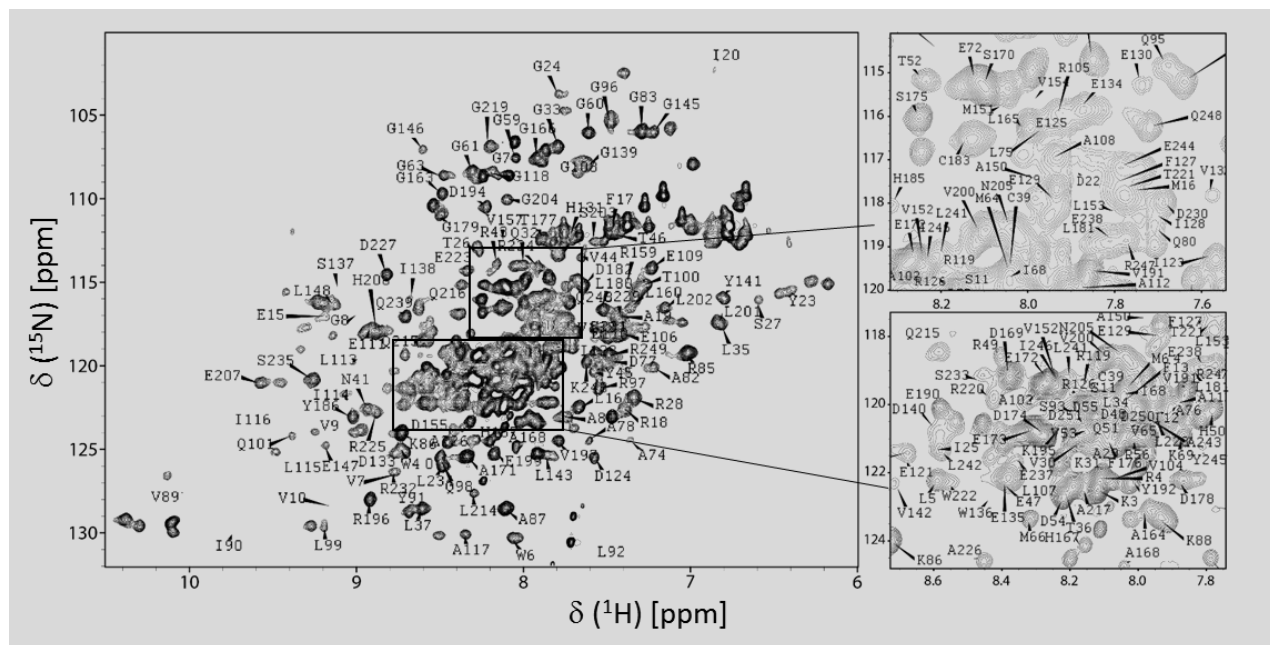


**Figure 1.**  $^1\text{H}$ - $^{15}\text{N}$ -HSQC spectrum of *Pa* TrmD. Cross peaks in the spectrum are labelled with residue name and sequence number.

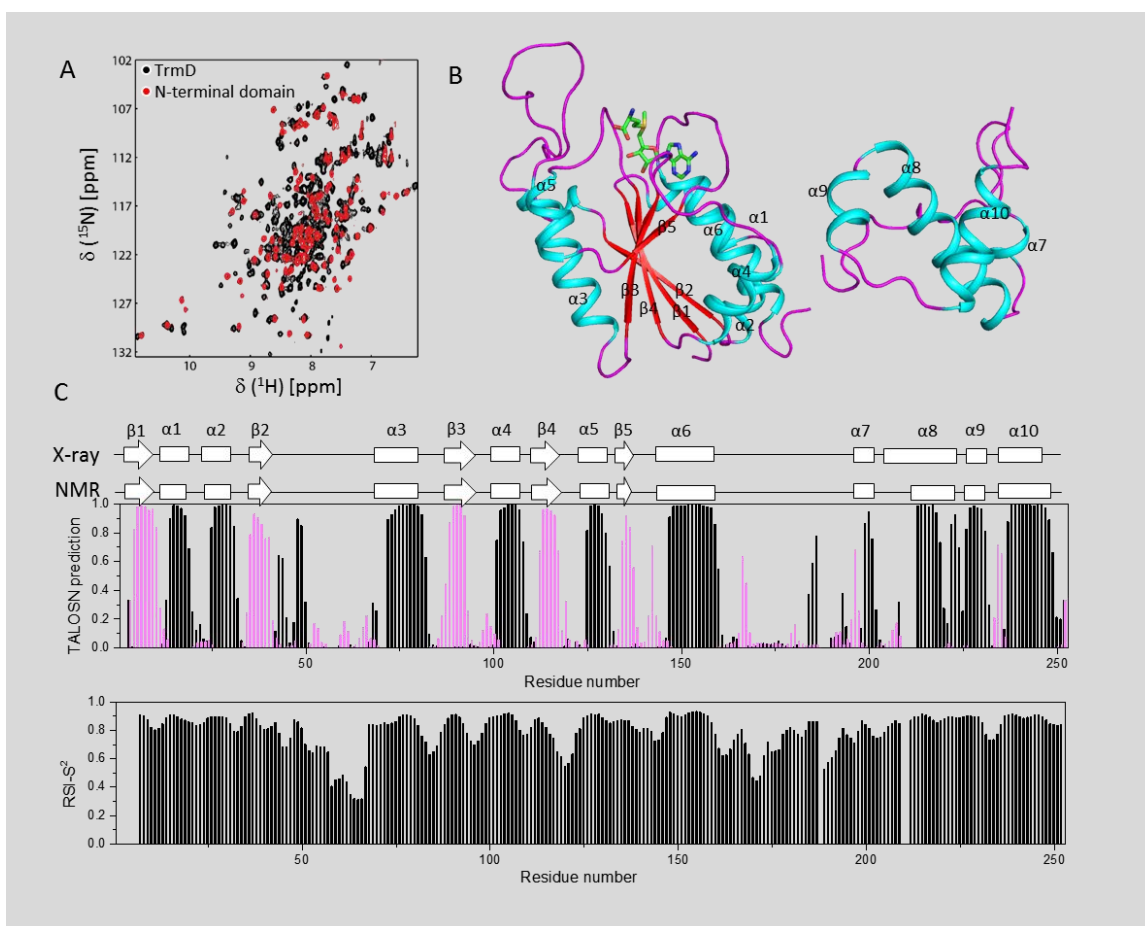


**Figure 2.** Secondary structure of *PaTrmD* in solution. **A.** Overlay of the  $^1\text{H}$ - $^{15}\text{N}$ -HSQC spectra of N-terminal domain (red) and full length *PaTrmD* (black). **B.** X-ray structure of the *PaTrmD* in complex with SAM. Only one monomer was shown (PDB accession code: 5WYQ). SAM is shown as ball and sticks. **C.** The secondary structures of *PaTrmD* in solution. The secondary structures and RCI- $S^2$  of assigned residues were obtained using TALOS+ and TALOS-N by analysing the assigned chemical shifts of backbone resonances. Residues predicted to form  $\alpha$  and  $\beta$  structures are shown with black and purple bars, respectively. The secondary structures of *PaTrmD* in solution were compared with those of the crystallographic structure of full-length *PaTrmD* (PDB accession code: 5WYQ).

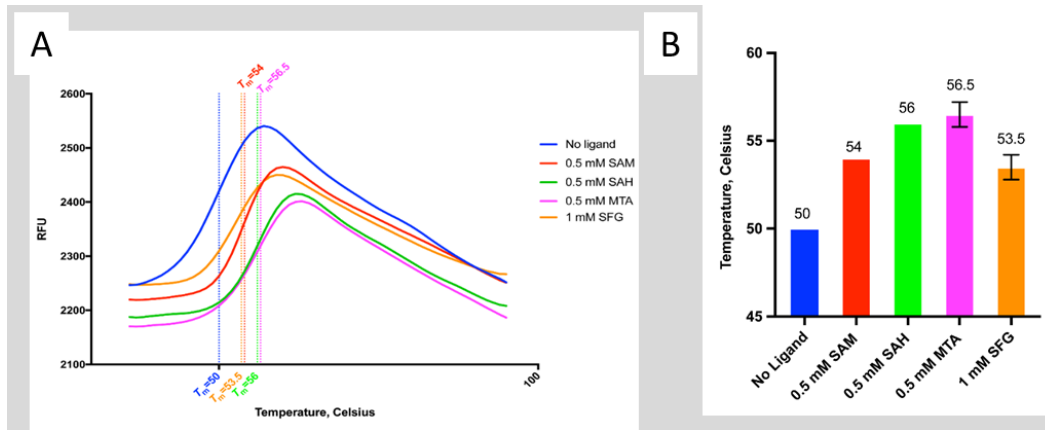


**Figure 3.** Thermal shift assay results for full-length *PaTrmD*. The thermal stabilities of *PaTrmD* in the absence and presence of SAM (0.5 mM), SAH (0.5 mM), MTA (0.5 mM) or Sinefungin (1 mM) were measured. The thermal denaturation curves are compared and the shifts in thermal stability are indicated by dotted lines (**A**). The  $T_m$  values of the *PaTrmD* and complexes are summarized (**B**). Plotted are mean  $\pm$  SD for the experiment done in duplicate.

## References

- Bjork, G., P. Wikstrom & A. Bystrom (1989) Prevention of translational frameshifting by the modified nucleoside 1-methylguanosine. *Science*, 244, 986-989.
- Delaglio, F., S. Grzesiek, G. W. Vuister, G. Zhu, J. Pfeifer & A. Bax (1995) NMRPipe: a multidimensional spectral processing system based on UNIX pipes. *J Biomol NMR*, 6, 277-93.
- Gayen, S., Q. Li & C. Kang (2012) The solution structure of the S4-S5 linker of the hERG potassium channel. *J Pept Sci*, 18, 140-5.
- Goto-Ito, S., T. Ito, M. Kuratani, Y. Bessho & S. Yokoyama (2009) Tertiary structure checkpoint at anticodon loop modification in tRNA functional maturation. *Nat Struct Mol Biol*, 16, 1109-15.
- Goto-Ito, S., T. Ito & S. Yokoyama (2017) Trm5 and TrmD: Two Enzymes from Distinct Origins Catalyze the Identical tRNA Modification, m(1)G37. *Biomolecules*, 7.
- Hill, P. J., A. Abibi, R. Albert, B. Andrews, M. M. Gagnon, N. Gao, T. Grebe, L. I. Hajec, J. Huang, S. Livchak, S. D. Lahiri, D. C. McKinney, J. Thresher, H. Wang, N. Olivier & E. T. Buurman (2013) Selective Inhibitors of Bacterial t-RNA-(N1G37) Methyltransferase (TrmD) That Demonstrate Novel Ordering of the Lid Domain. *Journal of Medicinal Chemistry*, 56, 7278-7288.
- Holmes, W. M., C. Andraos-Selim & M. Redlak (1995) tRNA-m1G methyltransferase interactions: Touching bases with structure. *Biochimie*, 77, 62-65.
- Ito, T., I. Masuda, K.-i. Yoshida, S. Goto-Ito, S.-i. Sekine, S. W. Suh, Y.-M. Hou & S. Yokoyama (2015) Structural basis for methyl-donor-dependent and sequence-specific binding to tRNA substrates by knotted methyltransferase TrmD. *Proceedings of the National Academy of Sciences*, 112, E4197-E4205.
- Johnson, B. A. (2004) Using NMRView to visualize and analyze the NMR spectra of macromolecules. *Methods Mol Biol*, 278, 313-52.
- Juhling, F., M. Morl, R. K. Hartmann, M. Sprinzl, P. F. Stadler & J. Putz (2009) tRNADB 2009: compilation of tRNA sequences and tRNA genes. *Nucleic Acids Res*, 37, D159-62.
- Kim, Y. M., Q. Li, H. Q. Ng, H. S. Yoon & C. Kang (2013) H, C and N chemical shift assignments for the N-terminal PAS domain of the KCNH channel from Zebrafish. *Biomol NMR Assign*.
- Li, Q., M. Raida & C. Kang (2010) <sup>1</sup>H, <sup>13</sup>C and <sup>15</sup>N chemical shift assignments for the N-terminal domain of the voltage-gated potassium channel-hERG. *Biomol NMR Assign*, 4, 211-3.
- Li, Y., Y. L. Wong, M. Y. Lee, H. Q. Ng & C. Kang (2016) Backbone assignment of the N-terminal 24-kDa fragment of Escherichia coli topoisomerase IV ParE subunit. *Biomol NMR Assign*, 10, 135-8.
- Li, Y., W. Zhong, A. Z. Koay, H. Q. Ng, X. Koh-Stenta, Q. Nah, S. H. Lim, A. Larsson, J. Lescar, J. Hill, P. C. Dedon & C. Kang (2018) Backbone resonance assignment for the N-terminal region of bacterial tRNA-(N1G37) methyltransferase. *Biomolecular NMR Assignments*.
- O'Dwyer, K., J. M. Watts, S. Biswas, J. Ambrad, M. Barber, H. Brulé, C. Petit, D. J. Holmes, M. Zalacain & W. M. Holmes (2004) Characterization of Streptococcus pneumoniae TrmD, a tRNA Methyltransferase Essential for Growth. *Journal of Bacteriology*, 186, 2346-2354.
- Persson, B. C., G. O. Bylund, D. E. Berg & P. M. Wikstrom (1995) Functional analysis of the ffh-trmD region of the Escherichia coli chromosome by using reverse genetics. *J Bacteriol*, 177, 5554-60.
- Pervushin, K., A. Ono, C. Fernandez, T. Szyperski, M. Kainosho & K. Wuthrich (1998) NMR scalar couplings across Watson-Crick base pair hydrogen bonds in DNA observed by transverse relaxation-optimized spectroscopy. *Proc Natl Acad Sci U S A*, 95, 14147-51.
- Salzmann, M., K. Pervushin, G. Wider, H. Senn & K. Wuthrich (1998) TROSY in triple-resonance experiments: new perspectives for sequential NMR assignment of large proteins. *Proc Natl Acad Sci U S A*, 95, 13585-90.
- Shen, Y. & A. Bax (2013) Protein backbone and sidechain torsion angles predicted from NMR chemical shifts using artificial neural networks. *Journal of Biomolecular NMR*, 56, 227-241.

- Shen, Y., F. Delaglio, G. Cornilescu & A. Bax (2009) TALOS+: a hybrid method for predicting protein backbone torsion angles from NMR chemical shifts. *J Biomol NMR*, 44, 213-23.
- Thanassi, J. A., S. L. Hartman-Neumann, T. J. Dougherty, B. A. Dougherty & M. J. Pucci (2002) Identification of 113 conserved essential genes using a high-throughput gene disruption system in *Streptococcus pneumoniae*. *Nucleic Acids Res*, 30, 3152-62.
- Thomas, S. R., C. A. Keller, A. Szyk, J. R. Cannon & N. A. LaRonde-LeBlanc (2011) Structural insight into the functional mechanism of Nep1/Emg1 N1-specific pseudouridine methyltransferase in ribosome biogenesis. *Nucleic Acids Research*, 39, 2445-2457.
- Zhang, Z., Y. Li, Y. R. Loh, W. W. Phoo, A. W. Hung, C. Kang & D. Luo (2016) Crystal structure of unlinked NS2B-NS3 protease from Zika virus. *Science*, 354, 1597-1600.
- Zhong, W., A. Koay, A. Ngo, Y. Li, Q. Nah, Y. H. Wong, Y. H. Chionh, H. Q. Ng, X. Koh-Stenta, A. Poulsen, K. Foo, M. McBee, M. L. Choong, A. El Sahili, C. Kang, A. Matter, J. Lescar, J. Hill & P. Dedon (2019) Targeting the Bacterial Epitranscriptome for Antibiotic Development: Discovery of Novel tRNA-(N(1)G37) Methyltransferase (TrmD) Inhibitors. *ACS Infect Dis*.